

SPECIFIC STAR FORMATION RATES TO REDSHIFT 5 FROM THE FORS DEEP FIELD AND THE GOODS-S FIELD¹

GEORG FEULNER^{2,3}, ARMIN GABASCH^{3,4}, MARA SALVATO⁴, NIV DRORY⁵, ULRICH HOPP^{3,4}, RALF BENDER^{3,4}

Accepted for publication in ApJL

ABSTRACT

We explore the build-up of stellar mass in galaxies over a wide redshift range $0.4 < z < 5.0$ by studying the evolution of the specific star formation rate (SSFR), defined as the star formation rate per unit stellar mass, as a function of stellar mass and age. Our work is based on a combined sample of ~ 9000 galaxies from the FORS Deep Field and the GOODS-S field, providing high statistical accuracy and relative insensitivity against cosmic variance. As at lower redshifts, we find that lower-mass galaxies show higher SSFRs than higher mass galaxies, although highly obscured galaxies remain undetected in our sample. Furthermore, the highest mass galaxies contain the oldest stellar populations at all redshifts, in principle agreement with the existence of evolved, massive galaxies at $1 < z < 3$. It is remarkable, however, that this trend continues to very high redshifts of $z \sim 4$. We also show that with increasing redshift the SSFR for massive galaxies increases by a factor of ~ 10 , reaching the era of their formation at $z \sim 2$ and beyond. These findings can be interpreted as evidence for an early epoch of star formation in the most massive galaxies, and ongoing star-formation activity in lower mass galaxies.

Subject headings: surveys — galaxies: evolution — galaxies: formation — galaxies: fundamental parameters — galaxies: high-redshift — infrared: galaxies

1. INTRODUCTION

In recent years, there has been considerable interest in the relation of the stellar mass in galaxies and their star-formation rate (SFR), since this allows to quantify the contribution of the recent star formation to the build up of stellar mass for different galaxy masses. Cowie et al. (1996) used K -band luminosities and [OII], $H\alpha$ or ultraviolet (UV) fluxes to investigate this connection for a K -selected sample of ~ 400 galaxies at $z < 1.5$ and noted an emerging population of massive, heavily star forming galaxies at higher redshifts, a phenomenon they termed ‘downsizing’. Later on, the ‘specific SFR’ (SSFR), defined as the SFR per unit stellar mass, was used to study this relation.

Guzman et al. (1997) derived the SSFR for 51 compact galaxies at $z < 1.4$ in the HDF flanking fields (Williams et al. 1996) finding no evidence for an increase of the peak SSFR with redshift. Brinchmann & Ellis (2000) studied 321 I -selected field galaxies at $z < 1$ and detected a clear upper limit on the SSFR moving to higher SFRs with increasing redshift. They conclude that the most massive galaxies must have formed the bulk of their stars before $z = 1$. Pérez-González et al. (2003) and Brinchmann et al. (2004) presented detailed investigations of the SSFR in the local universe, while Fontana et al. (2003) used a deep K -selected sample of

~ 300 galaxies in the HDF-S (Casertano et al. 2000) to trace the SSFR to $z > 2$ and found more evidence for higher SSFRs in the past, a result confirmed at $z < 1.5$ by Bauer et al. (2005) using spectroscopic data for ~ 350 galaxies. Juneau et al. (2005) found clear evidence for downsizing in a sample of ~ 200 galaxies at $0.8 < z < 2$ from the GDDS, and Feulner et al. (2005) used the MUNICS data (Drory et al. 2001; Feulner et al. 2003) to study the SSFR of ~ 6000 galaxies with photometric redshifts to $z = 1.2$, placing strong emphasis on the age of the stellar populations. They confirmed previous results on the rise of the SSFR with redshift, but found in addition that the highest mass galaxies are dominated by the oldest stellar populations at all redshifts.

Hammer et al. (2005) obtained $15\mu\text{m}$ fluxes for ~ 200 $z > 0.4$ galaxies and estimated that 15% of all $M_B < -20$ galaxies are luminous IR galaxies with SSFRs well above the range usually found using other star-formation estimators. Bell et al. (2005b) investigated ~ 1700 B -selected galaxies at $z \simeq 0.7$ with photometric redshifts, $\sim 25\%$ of which could be detected at $24\mu\text{m}$. They found that these galaxies typically have masses in the range $9.5 \lesssim M_\star \lesssim 11.0$ and SFRs of up to $\dot{\rho}_\star \lesssim 100 M_\odot \text{ yr}^{-1}$. Pérez-González et al. (2005) used about 8000 sources selected at $24\mu\text{m}$ to study the SSFR to $z \sim 3$, finding clear support for the downsizing picture.

In the following we present results on the SSFR of ~ 9000 galaxies at $0.4 < z < 5.0$ in the FORS Deep Field (FDF) and the GOODS-S field, reaching higher redshifts than previous investigations. This letter is organized as follows: We introduce the galaxy sample and our method to derive the SSFR in Section 2. In Section 3 we present our results on the evolution of the SSFR with redshift. Section 4 gives a brief account on the influence of dust attenuation. In Section 5 we discuss different evolutionary paths in the SSFR–stellar mass diagram, before we summarize our findings in Section 6. Throughout we as-

¹ Based on observations collected at the European Southern Observatory, Chile; proposal numbers 63.O-0005, 64.O-0149, 64.O-0158, 64.O-0229, 64.P-0150, 65.O-0048, 65.O-0049, 66.A-0547, 68.A-0013, and 69.A-0014. This work makes use of data obtained by the ESO GOODS/EIS project under Program ID LP168.A-0485.

² Email: feulner@usm.lmu.de

³ Universitäts-Sternwarte München, Scheinerstraße 1, D-81679 München, Germany

⁴ Max-Planck-Institut für Extraterrestrische Physik, Giessenbachstraße, D-85748 Garching bei München, Germany

⁵ University of Texas at Austin, Austin, Texas 78712

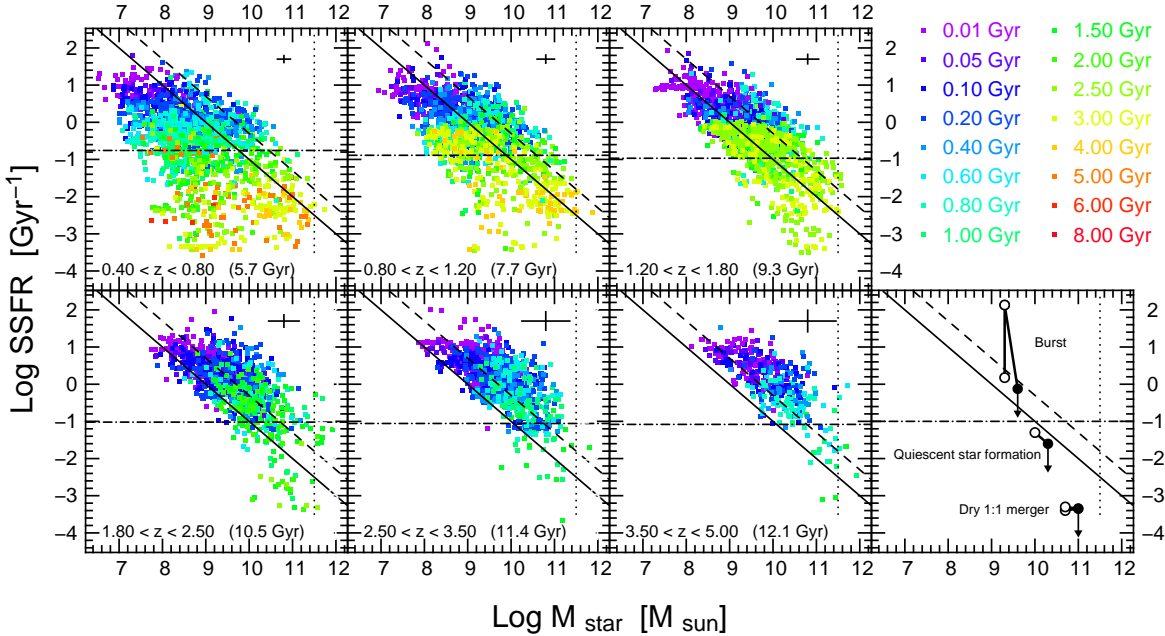


FIG. 1.— *Six panels to the left:* The SSFR as a function of stellar mass and redshift for the FDF and GOODS-S. Both the SFR and the mass are corrected for dust extinction. The solid and dashed lines correspond to SFRs of $1 M_{\odot} \text{ yr}^{-1}$ and $5 M_{\odot} \text{ yr}^{-1}$, respectively. Objects are colored according to the age of the main component of the stellar population synthesis model fit to the photometry, ranging from 0.01 Gyr (purple) to 8 Gyr (red). The dot-dashed line is the SSFR required to double a galaxy’s mass between each redshift epoch and today (assuming constant SFR); the corresponding look-back time is indicated in each panel. The error cross in each panel gives an idea of the typical errors, while the dotted line roughly represents the high-mass cut-off of the local stellar mass function (Drory et al. 2004; Fontana et al. 2004; Drory et al. 2005). *Lower right-hand panel:* Examples for evolutionary paths yielding a doubling of a galaxy’s mass, through quiescent star formation, through a burst of star formation superimposed on quiescent star formation, and through a dry equal-mass merger. Open symbols denote the starting point, filled symbols the final state; the doubling line is drawn for a lookback time of 10 Gyr ($z \approx 2$). The arrows indicated the influence of gas consumption or loss.

sume $\Omega_m = 0.3$, $\Omega_\Lambda = 0.7$ and $H_0 = 70 \text{ km s}^{-1} \text{ Mpc}^{-1}$. All magnitudes are in the Vega system.

2. THE GALAXY SAMPLES

The FDF (Heidt et al. 2003) offers photometry in the U , B , g , R , I , 834 nm, z , J and K bands and is complimented by deep spectroscopic observations (Noll et al. 2004). In this letter we use the I -selected sub-sample covering the deep central part of the field ($\sim 40 \text{ arcmin}^2$) as described in Gabasch et al. (2004a), containing 5557 galaxies down to $I = 26.4$.

Our K -band selected catalog for the GOODS-S field (Salvato et al., in prep.) is based on the publicly available $8.25 \times 2.5 \text{ arcmin}^2$ J , H , K_s VLT/ISAAC images and contains 3297 galaxies down to $K = 23.5$ in $\sim 50 \text{ arcmin}^2$. The U and I images are described in Arnouts et al. (2001), the B , V , and R images in Schirmer et al. (2003). The data were analyzed in a very similar way to the FDF data and already used in Gabasch et al. (2004b) and Drory et al. (2005). Although both samples in itself are not large in area, having two different lines of sight helps to overcome some of the effects of cosmic variance. Furthermore, we chose our redshift intervals large enough to further minimize the effect.

Photometric redshifts are derived using the method described in Bender et al. (2001). We estimate the SFRs of our galaxies from the spectral energy distribution by deriving the luminosity at $\lambda = 1500 \pm 100 \text{\AA}$ and converting it to an SFR as described in Madau et al. (1998) as-

suming a Salpeter initial mass function (Salpeter 1955). Although this is an extrapolation for the lower redshift bins, the results agree very well with our work at lower redshifts (Feulner et al. 2005). Stellar masses are computed from the multi-color photometry using the same method as in Drory et al. (2005). It is described in detail and tested against spectroscopic and dynamical mass estimates in Drory, Bender & Hopp (2004). In brief, we derive stellar masses by fitting a grid of stellar population synthesis models by Bruzual & Charlot (2003) with a range of star formation histories (SFHs), ages, metallicities and dust attenuations to the broad-band photometry. We describe the SFHs by a two-component model consisting of a main component with a smooth SFH $\propto \exp(-t/\tau)$ and a burst contributing up to 15% in mass. We allow SFH timescales $\tau \in [0.1, \infty]$ Gyr, metallicities $[\text{Fe}/\text{H}] \in [-0.6, 0.3]$, ages between 0.01 Gyr and the age of the universe at the objects’ redshift, and independent extinction values of $A_V \in [0.0, 1.5]$ for the main component and the burst, respectively. We adopt a Salpeter initial mass function for both components, with lower and upper mass cutoffs of 0.1 and $100 M_{\odot}$. The SFR is corrected with the dust attenuation obtained for the burst component using the extinction curve of Calzetti (1997). Note that at higher redshift the uncertainty in the mass estimate increases since the observed K band then probes the rest-frame blue or UV (Drory et al. 2005). We have verified the uncertainty in the mass estimate by comparing masses at lower redshifts from simulations with and without the NIR bands.

3. THE SPECIFIC STAR FORMATION RATE

One way to explore the contribution of star formation to the growth of stellar mass in galaxies of different mass is to study the redshift evolution of the specific SFR (SSFR; Guzman et al. 1997; Brinchmann & Ellis 2000) which is defined as the SFR per unit stellar mass. In Figure 1 we present the SSFR as a function of stellar mass and age for six different redshift bins covering the range $0.4 < z < 5.0$. We have convinced ourselves that the distributions of galaxies from the FDF and GOODS-S are in very good agreement.

Several effects can be observed in Fig. 1. The upper cut-off of the SSFR running essentially parallel to lines of constant SFR and shifting to higher SFRs with increasing redshift was already noted in earlier work (Brinchmann & Ellis 2000; Feulner et al. 2005; Bauer et al. 2005). This trend seems to continue to the highest redshifts probed by our sample: While at $z \sim 0.6$ we find $\text{SFR}_{\text{max}} \simeq 5 M_{\odot} \text{ yr}^{-1}$, galaxies reach as much as $\text{SFR}_{\text{max}} \simeq 100 M_{\odot} \text{ yr}^{-1}$ at $z \sim 4$. Note that this upper envelope is partly due to a selection effect: Heavily dust obscured star bursts cannot be detected in our sample (see, e.g., Hammer et al. 2005; Pérez-González et al. 2005), but our conclusions still hold for galaxies not heavily affected by dust extinction (see the discussion below). Furthermore, it is evident from the distribution of ages in this diagram, that the most massive galaxies contain the oldest stellar populations, as has been shown already in Feulner et al. (2005) and Drory et al. (2005). This is in agreement with the ‘downsizing’ scenario (Cowie et al. 1996)

4. THE ROLE OF DUST

The influence of dust extinction on the determination of the SSFR is two-fold. First, heavily dust enshrouded objects might escape detection because too much of the optical light is absorbed. Secondly, objects might be detected, but their SFR (and stellar mass) might be underestimated because of the increasing dust extinction in the UV. We try to correct for the second effect by including dust attenuation in our model fitting, and correcting both the SFR and the stellar mass accordingly, but the correction will likely be underestimated for extremely dusty objects. It is more complicated, of course, to overcome the first effect.

In principle both sources of uncertainty could be overcome with observations in the thermal infrared (IR), where the radiation absorbed by the dust component is re-emitted. Note however, that this approach suffers from confusion and identification problems and also involves uncertainties in the conversion of the observed IR flux to the total IR flux, and in the unknown contribution of dust heating by old stellar populations, see, e.g., the discussion in Bell et al. (2005b).

Luminous IR galaxies (LIRGs) are a well known population of dusty galaxies with very high SFRs and thus also SSFRs (see, e.g., Hammer et al. 2005; Pérez-González et al. 2005). They can be interpreted as galaxies experiencing a brief episode of heavy star formation triggered by mergers or gas infall. Due to their limited gas supply, these galaxies would spend most of their time in a ‘normal’ state with lower SSFR. Therefore, although our survey misses dust enshrouded star forming galaxies, they can be considered as intermittent

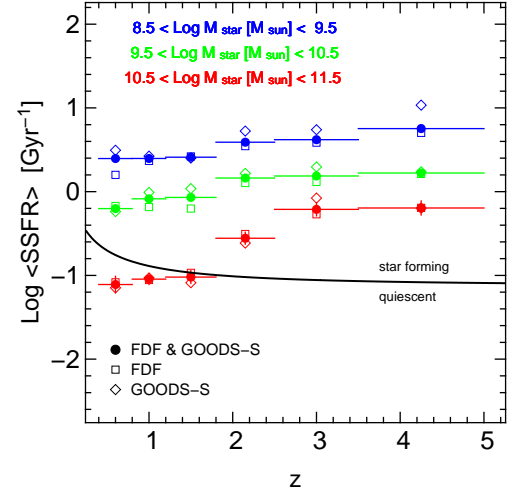


FIG. 2.— Average SSFRs for galaxies with stellar masses of $\log M_{\star}/M_{\odot} \in [8.5, 9.5]$ (blue), $[9.5, 10.5]$ (green) and $[10.5, 11.5]$ (red) and SFRs larger than $1 M_{\odot} \text{ yr}^{-1}$ as a function of z for FDF (open squares), GOODS-S (open diamonds) and the combined sample (filled circles). The error bar represents the error of the mean. All numbers are given in Table 1. The solid line indicates the doubling line of Fig. 1 which can be used to discriminate quiescent and heavily star forming galaxies.

stages in the evolution of galaxies. In particular our results on the existence of massive evolved galaxies even at high redshifts remain unaffected.

5. EVOLUTIONARY PATHS

In order to understand the role of various evolutionary paths in Fig. 1, it is helpful to visualize schematically different ways to double a galaxy’s mass as shown in the lower right-hand panel of Fig. 1. In the following we will discuss these paths in more detail.

Quiescently star-forming galaxies: A galaxy doubling its stellar mass by quiescent star formation at $0.5 M_{\odot} \text{ yr}^{-1}$ moves along a line of constant SFR towards the lower right part of the diagram. Note that galaxies below the doubling line in Fig. 1 do not have enough time to double their mass until today.

Starbursts: In contrast to a quiescent galaxy, a starburst can increase its mass in a shorter time interval, provided it has enough gas to consume. Bursts of star formation may be triggered by gas inflow or galaxy interactions, and quickly move a galaxy to high SSFRs, where it stays for a brief period of time before it fades back to ‘normal’ SSFRs. Given the typical dusty nature of starburst galaxies, they might escape detection in optical surveys during this stage. However, since these bursts are typically brief, the galaxies spend most of their time with the quiescent galaxies. Note that the exact path depends on the details of the star formation history during the burst phase, however, the only relevant parameter for the final mass is the mass of the consumed gas.

Dry mergers: Two galaxies undergoing a dry merger (i.e. without interaction-induced star formation) basically move to the right in the diagram. We illustrate this with equal stellar mass mergers; the stellar mass clearly doubles, while the final SSFR is the average of the two initial SSFRs.

Note that the ‘true’ endpoint of the galaxies’ evolution

TABLE 1
AVERAGE SSFRS OF GALAXIES AS A FUNCTION OF z

$\langle z \rangle$	log SSFR (1)	log SSFR (2)	log SSFR (3)
0.60	0.40 ± 0.04	-0.20 ± 0.03	-1.11 ± 0.10
1.00	0.40 ± 0.02	-0.09 ± 0.03	-1.04 ± 0.06
1.50	0.41 ± 0.02	-0.07 ± 0.02	-1.02 ± 0.08
2.15	0.59 ± 0.03	0.16 ± 0.03	-0.56 ± 0.07
3.00	0.62 ± 0.03	0.19 ± 0.02	-0.21 ± 0.08
4.25	0.75 ± 0.04	0.22 ± 0.04	-0.20 ± 0.08

NOTE. — The SSFR is given in units of Gyr $^{-1}$.
(1) $\log M_{\star}/M_{\odot} \in [8.5, 9.5]$. (2) $\log M_{\star}/M_{\odot} \in [9.5, 10.5]$. (3) $\log M_{\star}/M_{\odot} \in [10.5, 11.5]$.

will in all three cases likely be lower than shown, since all three processes diminish the limited gas supply. This is indicated by the down-ward pointing arrows.

In the light of these evolutionary possibilities it is obvious that the only two ways to form massive galaxies with old stellar populations is by highly efficient early star formation in massive haloes, or by dry merging of less massive galaxies harboring old stars. Both scenarios can, in principle, be distinguished by analyzing the redshift dependence of the SSFR in the most massive galaxies. The result is presented in Fig. 2, where we show the average SSFR as a function of redshift for galaxies in three mass intervals. At redshifts $z \lesssim 2$, the most massive galaxies with $\log M_{\star}/M_{\odot} \in [10.5, 11.5]$ are in a quiescent state with SSFRs not contributing significantly to their growth in stellar mass. However, at redshifts $z \gtrsim 2$, the picture changes dramatically: The SSFR for massive galaxies increases by a factor of ~ 10 until we witness the epoch of their formation at $z \sim 2$ and beyond. The fact that we miss galaxies at $z \gtrsim 1$ which have both high star-formation rate and mass, e.g. sub-mm galaxies at $z \sim 2$

(e.g. Smail et al. 2002), might shift this formation epoch to lower redshifts, but does not affect our conclusions.

6. DISCUSSION AND CONCLUSIONS

It is remarkable that the most massive galaxies show evidence of harboring the oldest stellar populations at all redshifts. Our sample shows this effect robustly out to very high redshifts of $z \sim 4$. Note that this is in agreement with the findings of massive, evolved galaxies in the population of Extremely Red Objects (EROs) at $1 < z < 2$ (Saracco et al. 2003; Cimatti et al. 2004; Saracco et al. 2005; Longhetti et al. 2005) and among the Distant Red Galaxies (DRGs) at $2 < z < 3$ (Labbé et al. 2005). Apparently this trend continues to even higher redshifts, indicating a very early formation epoch for the most massive galaxies in the universe, favoring the ‘downsizing’ picture (Cowie et al. 1996).

This important finding is evident in Fig. 2, where we show the average SSFR of galaxies with different masses as a function of redshift. While at redshifts $z \lesssim 2$ the most massive galaxies are in a quiescent state, at redshifts $z \gtrsim 2$ the SSFR for massive galaxies increases by a factor of ~ 10 reaching the epoch of their formation at $z \sim 2$ and beyond. While there is evidence for dry merging in the field galaxy population (Faber et al. 2005; Bell et al. 2005a), this strong increase in the SSFR of the most massive galaxies suggests that at least part of this population was formed in a period of efficient star formation in massive haloes.

We thank the anonymous referee for his comments which helped to improve this Letter. We acknowledge funding by the DFG (SFB 375). This research has made use of NASA’s ADS Abstract Service.

REFERENCES

- Arnouts, S., et al. 2001, A&A, 379, 740
Bauer, A. E., Drory, N., Hill, G. J., & Feulner, G. 2005, ApJ, 621, L89
Bell, E. F., et al. 2005a, ApJ, submitted, astro-ph/0506425
Bell, E. F., et al. 2005b, ApJ, 625, 23
Bender, R., et al. 2001, in Deep Fields, ed. S. Cristiani, A. Renzini, & R. E. Williams (Springer), 96
Brinchmann, J., Charlot, S., White, S. D. M., Tremonti, C., Kauffmann, G., Heckman, T., & Brinkmann, J. 2004, MNRAS, 351, 1151
Brinchmann, J., & Ellis, R. S. 2000, ApJ, 536, L77
Bruzual, G., & Charlot, S. 2003, MNRAS, 344, 1000
Calzetti, D. 1997, AJ, 113, 162
Casertano, S., et al. 2000, AJ, 120, 2747
Cimatti, A., et al. 2004, Nature, 430, 184
Cowie, L. L., Songaila, A., Hu, E. M., & Cohen, J. G. 1996, AJ, 112, 839
Drory, N., Bender, R., Feulner, G., Hopp, U., Maraston, C., Snigula, J., & Hill, G. J. 2004, ApJ, 608, 742
Drory, N., Bender, R., & Hopp, U. 2004, ApJ, 616, L103
Drory, N., Feulner, G., Bender, R., Botzler, C. S., Hopp, U., Maraston, C., Mendes de Oliveira, C., & Snigula, J. 2001, MNRAS, 325, 550
Drory, N., Salvato, M., Gabasch, A., Bender, R., Hopp, U., Feulner, G., & Pannella, M. 2005, ApJ, 619, L131
Faber, S. M., et al. 2005, ApJ, submitted, astro-ph/0506044
Feulner, G., Bender, R., Drory, N., Hopp, U., Snigula, J., & Hill, G. J. 2003, MNRAS, 342, 605
Feulner, G., Goranova, Y., Drory, N., Hopp, U., & Bender, R. 2005, MNRAS, 358, L1
Fontana, A., et al. 2003, ApJ, 594, L9
Fontana, A., et al. 2004, A&A, 424, 23
Gabasch, A., et al. 2004a, A&A, 421, 41
Gabasch, A., et al. 2004b, ApJ, 616, L83
Guzman, R., Gallego, J., Koo, D. C., Phillips, A. C., Lowenthal, J. D., Faber, S. M., Illingworth, G. D., & Vogt, N. P. 1997, ApJ, 489, 559
Hammer, F., Flores, H., Elbaz, D., Zheng, X. Z., Liang, Y. C., & Cesarsky, C. 2005, A&A, 430, 115
Heidt, J., et al. 2003, A&A, 398, 49
Juneau, S., et al. 2005, ApJ, 619, L135
Labbé, I., et al. 2005, ApJ, 624, L81
Longhetti, M., et al. 2005, MNRAS, 361, 897
Madau, P., Pozzetti, L., & Dickinson, M. 1998, ApJ, 498, 106
Noll, S., et al. 2004, A&A, 418, 885
Pérez-González, P., et al. 2005, ApJ, in press, astro-ph/0505101
Pérez-González, P. G., Gil de Paz, A., Zamorano, J., Gallego, J., Alonso-Herrero, A., & Aragón-Salamanca, A. 2003, MNRAS, 338, 525
Salpeter, E. E. 1955, ApJ, 121, 161
Saracco, P., et al. 2005, MNRAS, 357, L40
Saracco, P., et al. 2003, A&A, 398, 127
Schirmer, M., Erben, T., Schneider, P., Pietrzynski, G., Gieren, W., Carpano, S., Micol, A., & Pierfederici, F. 2003, A&A, 407, 869
Smail, I., Ivison, R. J., Blain, A. W., & Kneib, J.-P. 2002, MNRAS, 331, 495
Williams, R. E., et al. 1996, AJ, 112, 1335